Ligand-centred Chemistry of Molybdenum Organoimides. Formation of C–C Bonds *via* Generation of Nitrogen Ylides, Stereospecific Conversion of an Allylimide into Alkylvinylimides, Liberation of Cyanoformate or Amino Acid Esters†

Shirley A. Fairhurst,[a] David L. Hughes,[a] Saad K. Ibrahim,[a] Marie-Laurence Abasq,[b] Jean Talarmin,[b] M. Arlete Queiros,[c] Antonio Fonseca[c] and Christopher J. Pickett*[,a]

[a] *The Nitrogen Fixation Laboratory, University of Sussex, Brighton BN1 9RQ, UK*

[b] *URA CNRS 322, Universite de Bretagne Occidentale, BP 809, 29285 Brest, France*

[c] *Departamento de Quimica, Escola de Ciencias, Universidade do Minho, Largo de Paco, 4719 Braga, Portugal*

The range of imides *trans*-[MoCl(NCHR^{1}R^2)(dppe)$_2$]$^+$ made from the nitride *trans*-[MoCl(N)(dppe)$_2$] (dppe = $Ph_2PCH_2CH_2PPh_2$, R^1 = H or organic group, R^2 = organic group) has been extended; deprotonation of the imide group at the α-carbon gives reactive alkenylamides which have nitrogen ylide character {Mo≡N$^+$–C$^-$HR} and these are attacked by electrophiles. Stepwise C_1 homologation of a methylimide to ethyl- and isopropyl-imides can be achieved by successive deprotonation and methylation steps. The crystal structure of the alkenylamide *trans*-[MoCl(NCHCO$_2$Me)(dppe)$_2$] has been determined, as has that of the imide produced directly from it by C-methylation, *trans*-[MoCl{NCH(Me)CO$_2$Me}(dppe)$_2$]$^+$. Deprotonation at the α-carbon of an allylimide complex gives a species which is regioselectively and stereospecifically attacked by electrophiles at the γ-carbon; when the electrophile is the proton the overall reaction corresponds to a 1,3-prototropic rearrangement of the allylimide to the *E*-methylvinylimide. Electroreduction of imides in the presence of a source of protons releases the free amine; in this way esters of the amino acids glycine and DL-alanine have been synthesised. Two protons can be removed by base from imides with electron-withdrawing ester substituents and free cyanoformate esters are released from the metal centre by substitution with dinitrogen or CO.

Transition-metal nitrides are potentially useful reagents for introducing nitrogen functions into organic molecules.[1] Complexes of the general type *trans*-[MX(N)(L–L)$_2$] [M = Mo or W; X = halide; L–L = 1,2-bis(di-aryl- or -alkylphosphino)ethane] are particularly attractive in this context because the nitride ligand is nucleophilic and the square-planar {M(L–L)$_2$} assembly is robust. Such nitrides can be prepared from dinitrogen complexes of the type *trans*-[M(N$_2$)$_2$(L–L)$_2$] either by cleavage of an N–N bond[2] or by reaction with trimethylsilyl azide.[3]

This paper focuses on the chemistry of the {Mo≡N$^+$–CH$_2$R} group in complexes formed by alkylation of one such nitride, *trans*-[MoCl(N)(dppe)$_2$] (dppe = $Ph_2PCH_2CH_2PPh_2$) by RCH$_2$I (R = H or organic substituent).[3] Pathways for the conversion of the methylimide group in *trans*-[MoCl(NMe)(dppe)$_2$]$^+$ into ligated cyanide, aminocarbyne, isocyanate, isothiocyanate, isoselenocyanate groups or its release as methylamine have been described[4] and a preliminary account of the synthesis of glycine and DL-alanine methyl esters from *trans*-[MoCl(NCH$_2$CO$_2$Me)(dppe)$_2$]$^+$ **1** has been given.[1] A mechanistic study suggested that *two* α-protons can be removed from **1** when this complex is treated with the methoxide ion.[5]

Results and Discussion

Synthesis of Organoimides from trans-[MoCl(N)(dppe)$_2$].—Primary alkyl iodides RCH$_2$I (R = H, Me, Pr^n, MeOCO, EtOCO or CH$_2$=CH) react with *trans*-[MoCl(N)(dppe)$_2$] in tetrahydrofuran (thf) to give cations *trans*-[MoCl(NCH$_2$R)(dppe)$_2$]$^+$, isolable as iodide or other salts. Data for all new compounds are given in the Experimental section. Under similar conditions, the secondary and tertiary iodides Me$_2$CHI and Me$_3$CI do not react to a measurable extent, but *trans*-[MoCl(NCHMe$_2$)(dppe)$_2$]$^+$ can be synthesised indirectly from the ethylimide *trans*-[MoCl(NEt)(dppe)$_2$]$^+$, see below.

Formation and Alkylation of Nitrogen Ylides trans-[MoCl(NCHR)(dppe)$_2$]: *Structures of* trans-[MoCl(NCHCO$_2$Me)(dppe)$_2$] *and its C-Methylated Derivative* trans-[MoCl{NCH(Me)CO$_2$Me}(dppe)$_2$]$^+$.—Triethylamine removes a proton from the cation *trans*-[MoCl(NCH$_2$CO$_2$Me)(dppe)$_2$]$^+$ **1** to give the neutral alkenylamide *trans*-[MoCl(NCHCO$_2$Me)(dppe)$_2$] **2**, the structure of which has been determined by X-ray crystallography, Fig. 1. Complex **2** has incipient carbanion character and reacts with methyl iodide at the α-carbon to form a C–C bond.[1] The structure of the methylated product *trans*-[MoCl(NCHMeCO$_2$Me)(dppe)$_2$]$^+$ **3** has also been confirmed by X-ray crystallography on two forms of the iodide salt (**3a** and **3b**, see Experimental section) and the structure of one is also shown in Fig. 1. The dimensions of the imide **3** are generally similar to those found for *trans*-[MoCl(NMe)(dppe)$_2$]$^+$, for example Mo–N in **3a** is 1.742(6) Å and that in the methylimide is 1.733(5) Å.[6]

The principal changes in the molecular dimensions of complex **2** upon C-methylation to produce **3** are as follows. The Mo–N shortens in accord with an increase in multiple-bond character whereas, the N–C bond lengthens consistent with a decrease in C=N double-bond character. The Mo–P bond lengthens as Mo to P back bonding is diminished by the overall

† *Supplementary data available:* see Instructions for Authors, *J. Chem. Soc., Dalton Trans.*, 1995, Issue 1, pp. xxv–xxx.

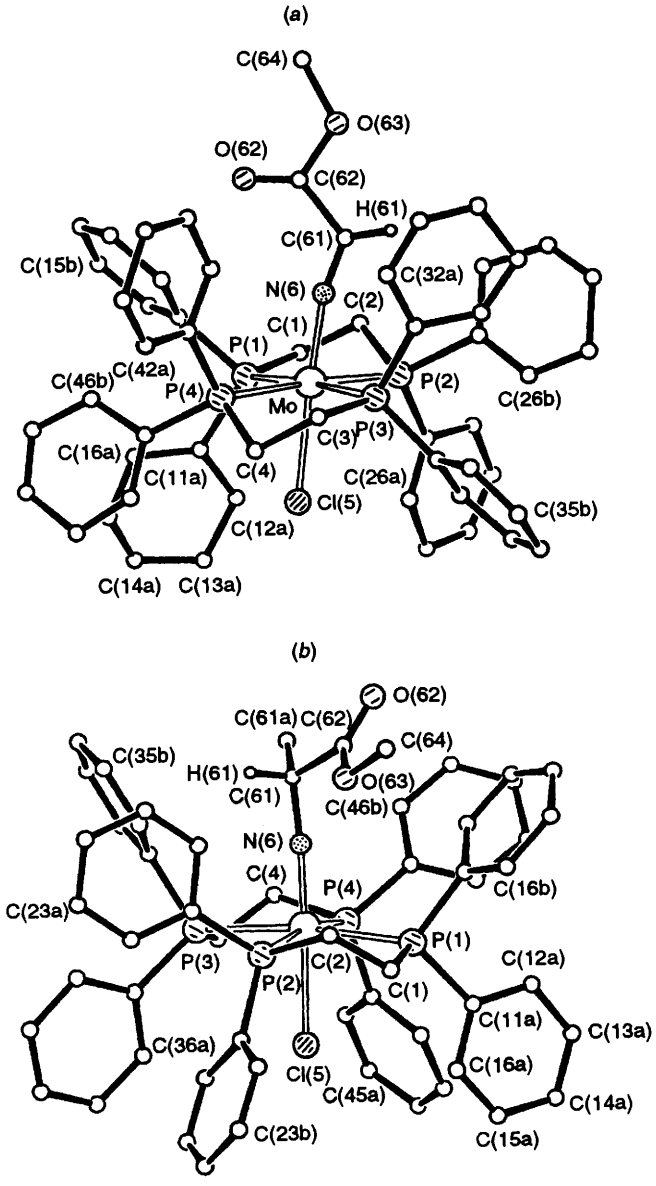

Fig. 1 (*a*) View of the molecule *trans*-[MoCl(NCHCO$_2$Me)(dppe)$_2$] **2**. (*b*) View of the cation *trans*-[MoCl{NCH(Me)CO$_2$Me}(dppe)$_2$]$^+$ of **3a**; that of **3b** is similar but has disorder in the imide ligand (see Experimental section). The atom numbering schemes are indicated

positive charge, whereas the Mo–Cl bond length is decreased. Similar changes have been documented for related systems.[6] A further difference between **2** and **3** is the alignment of the nitrogen ligands: in **2** the amide plane lies between the two phosphine ligands whereas in **3** (**a** or **b**) the ester group lies over one of the P–C–C–P linkages, *i.e.* perpendicular to the arrangement in **2**. The essentially planar conformation of the nitrogen ligand in **2**, together with the disposition of the substituent groups with respect to the dppe coligands, is discussed in the context of regioselective and stereospecific reactions described below. X-Ray structural data are given in Tables 1–4 and the syntheses of **1**–**3** are described in the Experimental section.

Removal of a proton from *trans*-[MoCl(NMe)(dppe)$_2$]$^+$ **4** requires a strong base. In earlier work it has been shown that treatment of **4** in thf with K[OBu^t] gives *trans*-[MoCl(NCH$_2$)(dppe)$_2$] **5**.[4] Although **5** has an extensive oxidation chemistry,[4] its reactions with carbon electrophiles has not been explored hitherto. Methyl iodide methylates **5** giving *trans*-[MoCl(NEt)(dppe)$_2$]$^+$ **6**; analogously, with *n*-propyl iodide, *trans*-[MoCl(NBu)(dppe)$_2$]$^+$ **7** is formed, Scheme 1.

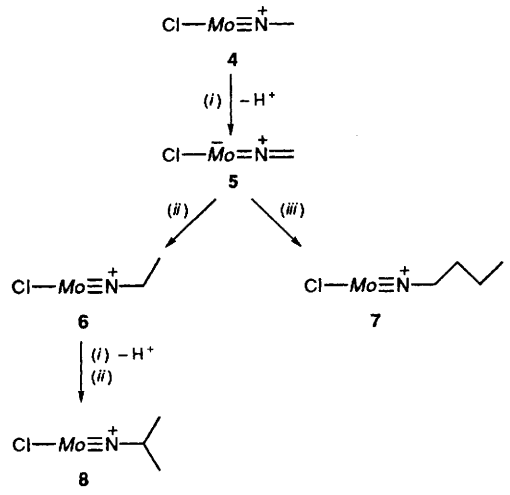

Scheme 1 Conversion of a methylimide to into ethyl-, butyl- and isopropyl-imides; *Mo* represents *trans*-{Mo(dppe)$_2$}. (*i*) Base; (*ii*) MeI; (*iii*) Pr^{n}I

The ethyl imide *trans*-[MoCl(NEt)(dppe)$_2$]$^+$ **6** also reacts with K[OBu^t] to generate a reactive ylide. The product *trans*-[MoCl(NCHMe)(dppe)$_2$] proved too sensitive to isolate in the solid state in a pure form but the following evidence shows that it is generated essentially quantitatively in thf solution. Addition of K[OBu^t] to a solution of 0.2 mol dm^{-3} [NBu$_4$][BF$_4$]–thf containing *trans*-[MoCl(NEt)(dppe)$_2$]$^+$ resulted in the disappearance of the voltammetric reduction peak for the parent cation and the appearance of a single new process corresponding to the oxidation of the deprotonated product. The peak oxidation potential $^{ox}E_p$ of this product was near to that observed for closely related **5**, Table 5. ^{31}P-{^{1}H} NMR spectroscopy in thf showed the disappearance of the resonance of *trans*-[MoCl(NEt)(dppe)$_2$]$^+$ on addition of the base and the appearance of a single new resonance. The chemical shift of the product is close to that of the methyleneamide analogue, Table 5. Finally, deprotonation of *trans*-[MoCl(NEt)(dppe)$_2$] followed by addition of MeI 'trapped' the ylide as the isopropylimide cation *trans*-[MoCl(NCHMe$_2$)(dppe)$_2$]$^+$ **8**, which was isolated and characterised as the iodide salt, Scheme 1.

Whereas the ethyl- or butyl-imide complexes **6** and **7** can be prepared directly from the parent nitride by reaction with the appropriate *n*-alkyl iodide, the isopropyl derivative **8** is not accessible by this route.

Cyclic voltammetric data show that complex **8** is also deprotonated by K[OBu^t] in thf to give a nitrogen ylide, Table 5, but attempts to extend the C_1 homologation to produce the *tert*-butylimide derivative failed. Bulky ligands do not coordinate to {M(dppe)$_2$} sites because of steric repulsion by the closely packed phenyl rings of the dppe ligands. The inability to form the *tert*-butyl derivative is presumably also a consequence of steric constraints.

1,3-Prototropic Rearrangement of an Allyl- to a Methylvinylimide Ligand; Regioselective and Stereospecific Attack by Electrophiles at the γ-Carbon of trans- [MoCl(N=CHCH=CH$_2$)(dppe)$_2$].—Deprotonation of the allylimide *trans*-[MoCl(NCH$_2$CH=CH$_2$)(dppe)$_2$]$^+$ **9** by K[OBu^t] in thf followed by reprotonation with HBF$_4$ does not lead to regeneration of the parent cation but to the formation of the methylvinylimide, *trans*-[MoCl(NCH=CHMe)(dppe)$_2$]$^+$ **10** by attack at the γ-carbon. The overall reaction can be viewed as a *1,3-prototropic* shift which proceeds *via trans*-[MoCl(N=CH-CH=CH$_2$)}(dppe)$_2$] **11**, Table 5. Treatment of **9** in thf with HBF$_4$ alone does not result in rearrangement.

Table 1 Final atomic coordinates (fractional × 10^4) for *trans*-[MoCl(NCHCO$_2$Me)(dppe)$_2$]·CH$_2$Cl$_2$ **2** with estimated standard deviations (e.s.d.s)

Atom	*x*	*y*	*z*	Atom	*x*	*y*	*z*
Mo[a]	2429.2(4)	1032(2)	2460.4(7)	C(34b)	1757(6)	−3370(9)	2386(9)
P(1)	3193(1)	2165(2)	3254(2)	C(35b)	1409(6)	−3067(9)	1658(9)
C(11a)	4042(5)	1902(8)	3334(6)	C(36b)	1379(5)	−2122(8)	1450(7)
C(12a)	4311(5)	1219(11)	3904(8)	C(3)	1863(5)	−216(7)	649(5)
C(13a)	4960(5)	920(11)	3921(9)	C(4)	2530(5)	93(7)	596(6)
C(14a)	5280(6)	1484(10)	3443(9)	P(4)	2640(1)	1269(2)	1079(1)
C(15a)	4989(6)	2012(11)	2923(7)	C(41a)	2153(4)	2020(6)	318(5)
C(16a)	4382(5)	2352(8)	2859(6)	C(42a)	2246(5)	2008(7)	−458(5)
C(11b)	3189(4)	3417(8)	2949(6)	C(43a)	1892(6)	2498(9)	−1032(6)
C(12b)	2812(5)	3715(8)	2279(6)	C(44a)	1359(6)	3070(9)	−854(7)
C(13b)	2839(5)	4688(9)	2093(8)	C(45a)	1278(6)	3072(9)	−77(8)
C(14b)	3198(6)	5321(9)	2576(9)	C(46a)	1658(4)	2519(7)	505(6)
C(15b)	3578(5)	5015(9)	3262(7)	C(41b)	3392(4)	1641(8)	947(6)
C(16b)	3548(5)	4089(7)	3458(6)	C(42b)	3886(5)	1099(11)	893(6)
C(1)	3047(5)	2251(8)	4268(6)	C(43b)	4473(6)	1282(15)	798(8)
C(2)	2429(5)	1918(7)	4314(6)	C(44b)	4574(6)	2263(14)	762(8)
P(2)	2278(1)	727(2)	3855(2)	C(45b)	4143(6)	2897(11)	813(6)
C(21a)	2787(4)	48(8)	4610(5)	C(46b)	3531(5)	2603(8)	870(6)
C(22a)	2673(5)	11(9)	5385(6)	Cl(5)[a]	3288(2)	−142(3)	2445(2)
C(23a)	3086(7)	−480(9)	5984(7)	N(6)[a]	1752(4)	1833(6)	2436(5)
C(24a)	3562(6)	−900(11)	5820(8)	C(61)[a]	1254(6)	2209(11)	2475(7)
C(25a)	3687(5)	−943(10)	5077(7)	C(62)[a]	1112(6)	3228(9)	2198(7)
C(26a)	3263(5)	−484(9)	4483(7)	O(62)[a]	1451(5)	3779(7)	2031(6)
C(21b)	1504(5)	344(10)	4034(6)	O(63)[a]	473(4)	3429(8)	2210(6)
C(22b)	1050(5)	1058(12)	4078(7)	C(64)[a]	287(13)	4456(15)	2112(15)
C(23b)	473(7)	606(13)	4172(11)	Cl(71)[a]	3812(3)	−2609(5)	3488(7)
C(24b)	358(7)	−220(21)	4209(10)	C(7)[a]	4448(8)	−1984(18)	3171(10)
C(25b)	845(7)	−982(12)	4184(7)	Cl(72)[a]	4927(3)	−1743(8)	4018(6)
C(26b)	1407(5)	−616(12)	4083(6)	Mo'[b]	2505(2)	901(6)	2475(3)
P(3)	1730(1)	−191(2)	1690(1)	Cl(5')[b]	1620(4)	2130(6)	2474(6)
C(31a)	918(4)	72(6)	1547(5)	N(6')[b]	3241(12)	287(20)	2606(16)
C(32a)	612(5)	743(8)	1086(6)	C(61')[b]	3795(11)	−325(19)	2656(16)
C(33a)	5(5)	934(10)	1028(7)	C(62')[b]	3933(28)	−1141(49)	2706(38)
C(34a)	−336(6)	647(9)	1497(7)	O(62')[b]	3470(11)	−1833(18)	2954(15)
C(35a)	−71(5)	−126(8)	2050(8)	O(63')[b]	4415(11)	−1473(18)	2740(15)
C(36a)	537(5)	−305(9)	2040(7)	C(64')[b]	4446(17)	−2780(29)	2867(24)
C(31b)	1768(4)	−1464(7)	1928(6)	Cl(71')[b]	1009(20)	4520(36)	1733(26)
C(32b)	2119(5)	−1784(8)	2670(6)	C(7')[b]	302(15)	4371(25)	1925(21)
C(33b)	2105(6)	−2733(10)	2890(8)	Cl(72')[b]	122(26)	4110(50)	1322(35)

[a] Site occupancy factor (s.o.f.) 0.80. [b] s.o.f. 0.20.

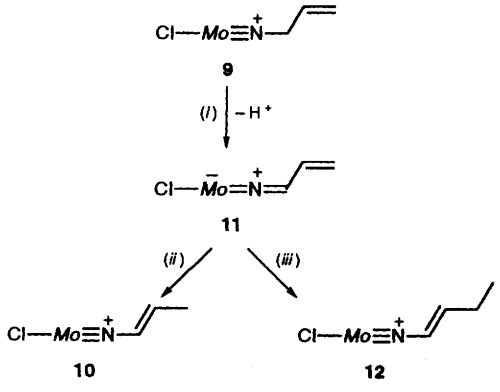

Scheme 2 Conversion of an allylimide to methyl- or ethyl-vinylimides; *Mo* represents *trans*-{Mo(dppe)$_2$}. (*i*) Base; (*ii*) H$^+$; (*iii*) MeI

Compounds **9** and **10** are easily distinguished electrochemically. Cyclic voltammetry shows that the vinyl product resulting from deprotonation/reprotonation of **9** is some 300 mV easier to reduce than is the parent allylimide and that its reduction is partially reversible at room temperature: reversibility in the reduction of **9** is only observed at temperatures below −10 °C. Presumably the lower energy of the lowest unoccupied molecular orbital (LUMO) of **10** and the greater stability of the anion is a consequence of metal–ligand π* character delocalised across the MoNCC framework. The voltammetry shows that the regioselectivity is greater than 90%, Scheme 2 and Fig. 2.

The proton NMR spectrum of the product *trans*-[MoCl(NCH=CHMe)}(dppe)$_2$]$^+$ **10** shows that the *E* isomer is exclusively formed. The coupling constant ^3J(CH=CH) is 15 Hz which is characteristic of protons in the *E* configuration. Confirmation of this stereochemistry was obtained by simulations of the ethylenic region of the ^{1}H NMR spectrum. ^3J(CH=CH) for *Z* isomers are typically in the region of 8 Hz; taking this value gives a calculated spectrum for the β proton which is essentially a quintet rather than the sextuplet actually observed. Iterative simulation gives a resonance pattern in excellent agreement with the experimental spectrum with ^3J(CH=CH) = 15 Hz, Fig. 3.

The reaction of complex **11** with MeI similarly produces the ethylvinylimide cation *trans*-[MoCl(NCH=CHEt)}(dppe)$_2$]$^+$ **12** by electrophilic attack at the γ-carbon. Again cyclic voltammetry and ^{1}H NMR spectroscopy show that the reaction is regiospecific and that the imide ligand also adopts the *E* configuration, Scheme 2. Electrophilic attack at either the α- or γ-carbons is consistent with carbanion character contributing to the resonance structure of **11**, as represented by the canonical forms in Scheme 3. As discussed below, the regioselectivity and stereospecificity of the reactions are closely linked: stereospecificity will be considered first.

The formation of the *E* isomers of the alkylvinylimides **10** and **12** must originate from steric constraints imposed by the dppe ligands. Maximisation of π-orbital interactions within the

Table 2 Selected bond distances (Å) and angles (°) for *trans*-[MoCl(NCHCO$_2$Me)(dppe)$_2$]·CH$_2$Cl$_2$ **2** with e.s.d.s. in parentheses

(*a*) About the Mo atom			
Mo–P(1)	2.508(3)	Mo′–P(1)	2.533(7)
Mo–P(2)	2.515(3)	Mo′–P(2)	2.524(5)
Mo–P(3)	2.500(3)	Mo′–P(3)	2.480(7)
Mo–P(4)	2.522(3)	Mo′–P(4)	2.521(5)
Mo–Cl(5)	2.503(4)	Mo′–Cl(5′)	2.592(11)
Mo–N(6)	1.853(8)	Mo′–N(6′)	1.800(26)
P(1)–Mo–P(2)	77.8(1)	P(1)–Mo′–P(2)	77.2(2)
P(1)–Mo–P(3)	175.7(1)	P(1)–Mo′–P(3)	173.1(3)
P(2)–Mo–P(3)	101.9(1)	P(2)–Mo′–P(3)	102.2(2)
P(1)–Mo–P(4)	101.6(1)	P(1)–Mo′–P(4)	101.0(3)
P(2)–Mo–P(4)	176.4(1)	P(2)–Mo′–P(4)	172.3(4)
P(3)–Mo–P(4)	78.4(1)	P(3)–Mo′–P(4)	78.8(2)
P(1)–Mo–Cl(5)	90.2(1)	P(1)–Mo′–Cl(5′)	84.2(3)
P(2)–Mo–Cl(5)	97.8(1)	P(2)–Mo′–Cl(5′)	77.4(3)
P(3)–Mo–Cl(5)	85.6(1)	P(3)–Mo′–Cl(5′)	88.9(2)
P(4)–Mo–Cl(5)	78.6(1)	P(4)–Mo′–Cl(5′)	95.1(3)
P(1)–Mo–N(6)	94.1(3)	P(1)–Mo′–N(6′)	81.2(9)
P(2)–Mo–N(6)	82.7(3)	P(2)–Mo′–N(6′)	99.8(9)
P(3)–Mo–N(6)	90.1(2)	P(3)–Mo′–N(6′)	105.7(9)
P(4)–Mo–N(6)	100.9(3)	P(4)–Mo′–N(6′)	87.2(9)
Cl(5)–Mo–N(6)	175.7(3)	Cl(5′)–Mo′–N(6′)	165.4(9)
(*b*) In the dppe ligands			
P(1)–C(11a)	1.870(10)	P(3)–C(31a)	1.781(9)
P(1)–C(11b)	1.835(11)	P(3)–C(31b)	1.833(10)
P(1)–C(1)	1.833(11)	P(3)–C(3)	1.863(10)
C(1)–C(2)	1.444(15)	C(3)–C(4)	1.541(15)
C(2)–P(2)	1.851(10)	C(4)–P(4)	1.844(11)
P(2)–C(21a)	1.806(10)	P(4)–C(41a)	1.847(9)
P(2)–C(21b)	1.857(11)	P(4)–C(41b)	1.781(10)
Mo–P(1)–C(11a)	117.4(4)	Mo–P(3)–C(31a)	114.8(3)
Mo–P(1)–C(11b)	119.3(3)	Mo–P(3)–C(31b)	123.8(3)
Mo–P(1)–C(1)	109.6(4)	Mo–P(3)–C(3)	109.0(3)
Mo′–P(1)–C(11a)	112.2(4)	Mo′–P(3)–C(31a)	120.2(3)
Mo′–P(1)–C(11b)	123.6(3)	Mo′–P(3)–C(31b)	119.1(3)
Mo′–P(1)–C(1)	110.5(4)	Mo′–P(3)–C(3)	108.3(3)
C(11a)–P(1)–C(11b)	99.2(5)	C(31a)–P(3)–C(31b)	103.6(4)
C(11a)–P(1)–C(1)	107.3(4)	C(31a)–P(3)–C(3)	102.1(4)
C(11b)–P(1)–C(1)	102.5(5)	C(31b)–P(3)–C(3)	100.7(5)
P(1)–C(1)–C(2)	111.7(7)	P(3)–C(3)–C(4)	112.2(6)
C(1)–C(2)–P(2)	111.2(8)	C(3)–C(4)–P(4)	105.5(7)
Mo–P(2)–C(2)	101.8(4)	Mo–P(4)–C(4)	105.8(4)
Mo–P(2)–C(21a)	126.5(4)	Mo–P(4)–C(41a)	123.7(3)
Mo–P(2)–C(21b)	119.9(3)	Mo–P(4)–C(41b)	120.0(3)
Mo′–P(2)–C(2)	105.0(4)	Mo′–P(4)–C(4)	102.4(4)
Mo′–P(2)–C(21a)	121.1(4)	Mo′–P(4)–C(41a)	129.1(4)
Mo′–P(2)–C(21b)	122.3(3)	Mo′–P(4)–C(41b)	117.6(3)
C(2)–P(2)–C(21a)	98.0(5)	C(4)–P(4)–C(41a)	100.8(4)
C(2)–P(2)–C(21b)	106.6(6)	C(4)–P(4)–C(41b)	104.4(5)
C(21a)–P(2)–C(21b)	100.5(5)	C(41a)–P(4)–C(41b)	99.2(5)
(*c*) In the amide ligand			
N(6)–C(61)	1.224(16)	N(6′)–C(61′)	1.47(4)
C(61)–C(62)	1.522(20)	C(61′)–C(62′)	1.18(7)
C(62)–O(62)	1.145(17)	C(62′)–O(62′)	1.52(7)
C(62)–O(63)	1.429(16)	C(62′)–O(63′)	1.14(7)
O(63)–C(64)	1.500(24)	O(63′)–C(64′)	1.85(5)
Mo–N(6)–C(61)	167.5(10)	Mo′–N(6′)–C(61′)	172.2(21)
N(6)–C(61)–C(62)	121.2(13)	N(6′)–C(61′)–C(62′)	140(4)
C(61)–C(62)–O(62)	127.8(12)	C(61′)–C(62′)–O(62′)	118(5)
C(61)–C(62)–O(63)	108.7(11)	C(61′)–C(62′)–O(63′)	128(6)
O(62)–C(62)–O(63)	123.4(12)	O(62′)–C(62′)–O(63′)	112(5)
C(62)–O(63)–C(64)	115.7(14)	C(62′)–O(63′)–C(64′)	115(4)
(*d*) Selected torsion angles			
P(1)–C(1)–C(2)–P(2)	51.0(9)	N(6)–C(61)–C(62)–O(62)	−10.6(22)
P(3)–C(3)–C(4)–P(4)	−54.5(8)	N(6)–C(61)–C(62)–O(63)	172.1(12)
Mo–N(6)–C(61)–C(62)	−177(3)	C(61)–C(62)–O(63)–C(64)	168.3(14)

Table 3 Final atomic coordinates (fractional $\times 10^4$) for *trans*-[MoCl{NCH(Me)CO_2Me}(dppe)$_2$] I·2MeCN·solvent (thf?) **3a** with e.s.d.s in parentheses

Atom	*x*	*y*	*z*
I	5262.8(7)	1871.4(7)	543.2(5)
Mo	1647.4(5)	3790.0(5)	2848.3(3)
P(1)	1629(2)	2234(2)	2344(1)
C(11a)	702(7)	843(6)	2890(4)
C(12a)	−230(8)	469(7)	2672(5)
C(13a)	−962(9)	−538(9)	3146(7)
C(14a)	−807(10)	−1135(9)	3804(6)
C(15a)	124(9)	−754(8)	4001(5)
C(16a)	868(8)	222(7)	3555(5)
C(11b)	1395(7)	2479(7)	1429(4)
C(12b)	675(8)	3139(8)	1199(5)
C(13b)	378(8)	3247(9)	552(6)
C(14b)	803(10)	2714(10)	118(6)
C(15b)	1522(11)	2070(9)	326(6)
C(16b)	1799(8)	1956(8)	986(5)
C(1)	3034(7)	1984(7)	2252(5)
C(2)	3927(7)	3064(7)	1982(4)
P(2)	3687(2)	3712(2)	2672(1)
C(21a)	4789(7)	4990(7)	2287(5)
C(22a)	5379(8)	5329(8)	2726(5)
C(23a)	6187(10)	6329(9)	2433(7)
C(24a)	6369(10)	7016(9)	1695(7)
C(25a)	5792(8)	6693(8)	1252(5)
C(26a)	4991(7)	5692(7)	1548(5)
C(21b)	4163(6)	2874(7)	3440(4)
C(22b)	4907(8)	2240(8)	3331(6)
C(23b)	5303(10)	1653(9)	3911(7)
C(24b)	4915(10)	1681(10)	4604(7)
C(25b)	4180(8)	2309(8)	4731(5)
C(26b)	3816(7)	2914(7)	4137(4)
P(3)	1664(2)	5134(2)	3521(1)
C(31a)	2350(7)	5053(7)	4261(4)
C(32a)	3350(8)	5818(8)	4131(6)
C(33a)	3885(9)	5712(9)	4717(7)
C(34a)	3453(10)	4880(10)	5388(6)
C(35a)	2475(9)	4149(8)	5508(5)
C(36a)	1929(8)	4236(8)	4951(5)
C(31b)	2140(7)	6608(6)	2917(4)
C(32b)	1566(9)	7372(8)	3012(6)
C(33b)	1966(11)	8462(9)	2537(7)
C(34b)	2926(10)	8788(8)	1986(7)
C(35b)	3478(10)	8067(8)	1892(6)
C(36b)	3110(8)	6951(7)	2358(5)
C(3)	196(7)	4942(7)	3994(4)
C(4)	−529(7)	4873(7)	3474(5)
P(4)	−460(2)	3616(2)	3266(1)
C(41a)	−1312(7)	2483(7)	4131(5)
C(42a)	−1341(7)	1398(7)	4210(5)
C(43a)	−2047(8)	559(8)	4820(5)
C(44a)	−2714(8)	760(9)	5374(5)
C(45a)	−2655(8)	1813(9)	5313(5)
C(46a)	−1976(7)	2687(8)	4693(5)
C(41b)	−1349(7)	3625(8)	2639(4)
C(42b)	−1717(9)	2660(8)	2518(6)
C(43b)	−2344(9)	2610(10)	2030(6)
C(44b)	−2623(8)	3532(11)	1653(5)
C(45b)	−2319(10)	4499(12)	1759(6)
C(46b)	−1687(9)	4511(9)	2256(6)
Cl(5)	1288(2)	2387(2)	4086(1)
N(6)	1893(6)	4837(5)	1986(3)
C(61)	2114(10)	5758(8)	1301(5)
C(61a)	1227(12)	6390(11)	1296(6)
C(62)	2341(8)	5460(7)	611(5)
O(62)	1922(6)	5739(6)	117(4)
O(63)	3134(5)	4930(5)	639(3)
C(64)	3533(8)	4719(8)	−30(5)
The solvent molecules			
N(7)	950(19)	2626(16)	7748(15)
C(7)	497(26)	1763(26)	8285(19)
C(71)	−34(36)	791(21)	8865(13)
N(8)[a]	4176(20)	1660(18)	6585(10)
C(8a)[b]	4438(61)	660(47)	7081(37)
N(8a)[b]	4997(44)	128(36)	7289(30)
C(8b)[b]	4464(75)	1025(44)	6988(29)
C(81b)[b]	4368(52)	208(36)	7752(23)
C(8c)[b]	4040(60)	1029(46)	7121(17)
C(81c)[b]	3760(41)	391(33)	7933(14)
C(9)[c]	−1868(41)	360(42)	658(27)
C(91)[c]	−2054(36)	1524(37)	675(23)
C(95)[d]	3237(26)	117(25)	9937(17)
C(96)[d]	3691(25)	378(24)	9695(16)

[a] s.o.f. 0.8. [b] s.o.f. 0.3. [c] s.o.f. 0.4. [d] s.o.f. 0.5.

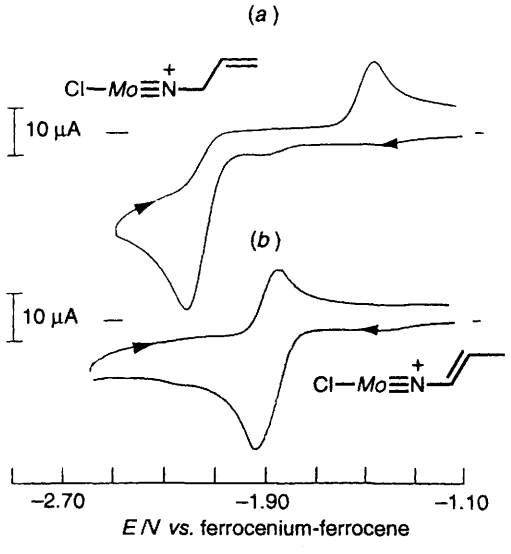

Fig. 2 Cyclic voltammograms of (*a*) the allyl complex **9** and (*b*) the methylvinyl product **10**. Recorded in thf–0.2 mol dm^{-3} [NBu_4][BF_4] at a vitreous carbon electrode, scan rate 100 mV s^{-1}. At −25 °C the reduction of **9** appears partially reversible. Note trace of **10** in voltammogram (*a*) and **9** in (*b*)

precursor complex **11** requires planarity of the {Mo–N=CHCH=CH_2} moiety, just as is observed for the {Mo–N=CHC=O(OMe)} group in **2**, Fig. 1. If we assume that the dppe ligands in **11** are arranged about the Mo in a similar fashion to that in **2**, then two planar configurations of the amide ligand in **11** with respect to these coligands can be envisaged; these are represented in Scheme 4 (**a** and **b**). The *Z* arrangement directs the larger {CH_2} substituent group on the β-carbon towards the phenyl groups of the dppe ligand, Scheme 4(**a**). In contrast, adoption of the *E* configuration places this group in the *exo* position with the smaller H substituent on the β-carbon now directed towards the phenyl groups, Scheme 4(**b**). With the latter arrangement steric repulsions are clearly minimised. Electrophilic attack on the γ-carbon of **11** with the alkenylamide group locked in the *E* configuration would give exclusively the *E* product, as is experimentally observed, Scheme 2.

Some indication of the importance of such steric interactions in determining the orientation of substituent groups is evident from the crystal structure of complex **2**. The O atom on the β-carbon, O(62), is directed towards the phenyl ligands, whereas the larger MeO group occupies the *exo* position and is well clear of phenyl-group contacts. Note that even with this arrangement steric repulsion appears to result in some tilting of the rigid, planar NCHCO_2Me group away from the phenyl rings, Fig. 1(*a*). The crystal structure of *trans*-[MoCl(NCHMeCO_2Me)-

Table 4 Selected molecular bond distances (Å) and angles (°) in *trans*-[MoCl{NCH(Me)CO_2Me}(dppe)$_2$]I·2MeCN·solvent **3a** with e.s.d.s in parentheses

(*a*) About the Mo atom			
Mo–P(1)	2.559(3)	Mo–P(4)	2.576(2)
Mo–P(2)	2.555(2)	Mo–Cl(5)	2.443(2)
Mo–P(3)	2.542(3)	Mo–N(6)	1.742(6)
P(1)–Mo–P(2)	79.5(1)	P(3)–Mo–Cl(5)	84.4(1)
P(1)–Mo–P(3)	172.0(1)	P(4)–Mo–Cl(5)	82.6(1)
P(2)–Mo–P(3)	98.7(1)	P(1)–Mo–N(6)	95.0(3)
P(1)–Mo–P(4)	100.6(1)	P(2)–Mo–N(6)	93.9(2)
P(2)–Mo–P(4)	169.6(1)	P(3)–Mo–N(6)	92.9(3)
P(3)–Mo–P(4)	79.8(1)	P(4)–Mo–N(6)	96.5(2)
P(1)–Mo–Cl(5)	87.7(1)	Cl(5)–Mo–N(6)	177.2(3)
P(2)–Mo–Cl(5)	87.0(1)		
(*b*) In the dppe ligands			
P(1)–C(11a)	1.844(7)	P(3)–C(31a)	1.817(10)
P(1)–C(11b)	1.821(9)	P(3)–C(31b)	1.840(7)
P(1)–C(1)	1.844(9)	P(3)–C(3)	1.844(8)
C(2)–P(2)	1.840(10)	C(4)–P(4)	1.847(10)
P(2)–C(21a)	1.820(7)	P(4)–C(41a)	1.845(7)
P(2)–C(21b)	1.834(9)	P(4)–C(41b)	1.820(10)
Mo–P(1)–C(11a)	120.4(3)	Mo–P(3)–C(31a)	123.2(3)
Mo–P(1)–C(11b)	118.3(3)	Mo–P(3)–C(31b)	115.1(3)
C(11a)–P(1)–C(11b)	102.0(4)	C(31a)–P(3)–C(31b)	103.4(4)
Mo–P(1)–C(1)	106.5(3)	Mo–P(3)–C(3)	106.0(3)
C(11a)–P(1)–C(1)	103.2(4)	C(31a)–P(3)–C(3)	102.3(4)
C(11b)–P(1)–C(1)	104.4(4)	C(31b)–P(3)–C(3)	104.7(4)
Mo–P(2)–C(2)	104.6(3)	Mo–P(4)–C(4)	103.9(3)
Mo–P(2)–C(21a)	119.9(3)	Mo–P(4)–C(41a)	119.4(3)
C(2)–P(2)–C(21a)	103.9(4)	C(4)–P(4)–C(41a)	103.4(4)
Mo–P(2)–C(21b)	120.8(2)	Mo–P(4)–C(41b)	121.6(3)
C(2)–P(2)–C(21b)	103.6(4)	C(4)–P(4)–C(41b)	103.9(5)
C(21a)–P(2)–C(21b)	101.7(4)	C(41a)–P(4)–C(41b)	102.4(4)
(*c*) In the imide ligand			
N(6)–C(61)	1.434(10)	C(62)–O(62)	1.182(13)
C(61)–C(61a)	1.506(20)	C(62)–O(63)	1.316(13)
C(61)–C(62)	1.530(15)	O(63)–C(64)	1.455(13)
Mo–N(6)–C(61)	175.6(7)	C(61)–C(62)–O(62)	124.7(10)
N(6)–C(61)–C(61a)	112.4(8)	C(61)–C(62)–O(63)	108.6(9)
N(6)–C(61)–C(62)	114.0(9)	O(62)–C(62)–O(63)	126.5(10)
C(61a)–C(61)–C(62)	111.2(10)	C(62)–O(63)–C(64)	114.3(8)
(*d*) Selected torsion angles			
P(1)–C(1)–C(2)–P(2)	61.1(7)	N(6)–C(61)–C(62)–O(62)	132.3(10)
P(3)–C(3)–C(4)–P(4)	64.5(7)	C(61a)–C(61)–C(62)–O(62)	3.8(15)
Mo–N(6)–C(61)–C(62)	162(8)	C(61a)–C(61)–C(62)–O(63)	178.8(9)
Mo–N(6)–C(61)–C(61a)	−71(9)	C(61)–C(62)–O(63)–C(64)	−172.6(8)
N(6)–C(61)–C(62)–O(63)	−52.7(11)	O(62)–C(62)–O(63)–C(64)	2.3(14)

$(dppe)_2]^+$ **3a** shows that *both* O and OMe substituents on the β-carbon are free to orientate away from the phenyl rings, the α-carbon is saturated and the electronic restriction for π-delocalisation across the MoNCCO framework is lifted, Fig. 1(*b*).

That C–H or C–C bond formation occurs regioselectively at the γ-carbon can be explained in the following way. The two dppe ligands hinder lateral access to the α-carbon of the alkenylamide ligand of complex **11**: in the favoured *E* configuration, the *exo* γ-carbon is the 'first in line' of the two nucleophilic carbon centres with respect to attack by an electrophile from a nominally axial direction. Attack at the *exo*-carbon commits the system to irreversible formation of the alkylvinylimide product **10** or **12**.

The regioselective and stereospecific course of the above reactions shows some parallel with electrophilic attack on certain alkenyldiazenide complexes of tungsten reported by Hidai and co-workers.[8] For example, *trans*-[WF{N=N–C(Me)=CH_2}$(dppe)_2$] reacts with methyl iodide at the *exo*-methylene group to give the *E*-diazoalkane product *trans*-$[WF(NN{=}CMeEt)(dppe)_2]^+$ (*cf.* formation of the *E* isomer by γ-carbon methylation of **11**). Notably, methylation at the β-nitrogen (corresponding to the α-carbon in **11**) does not take place, although this type of reaction readily occurs with closely related alkyldiazenide complexes.[9] As far as we are aware, 1,3-prototropic shifts involving the interconversion of alkenylhydrazide and diazoalkane groups, *e.g.* NNH(CH=CH_2) ⟷ NN=CHMe, have yet to be observed.

Table 5 Primary redox potentials and $^{31}P-\{^1H\}$ NMR spectral data for imide complexes and their ylide derivatives

trans-$[MoCl(NR)(dppe)_2]^+$ R	$E_{\frac{1}{2}}{}^a$/V		$^{31}P-\{^1H\}$ NMR[b]	
	Imide	Ylide[c]	Imide	Ylide[c]
4 Me	−2.30	−0.72	−97.4	−83.3
6 Et	−2.20	−1.0	−97.0	−82.3
8 Pr^i	−2.33	−1.16	−98.1	−81.4
9 $CH_2CH{=}CH_2$	−2.20	−0.92[d]	−96.8[d]	−84.3[d]
10 CH=CHMe	−1.89	−0.92[d]	−97.2[d]	−84.3[d]
12 CH=CHEt	−1.87	−0.90	−97.7	−84.3
1 CH_2CO_2Me	−2.12	−0.43	−98.0	−86.7
3 $CH(Me)CO_2Me$	−2.21	−0.65	−99.4	−90.8

[a] Reversible reduction potentials for the imides (Mo^{IV}–Mo^{III}) and oxidation potentials for the conjugate ylides (Mo^{II}–Mo^{III}) both relative to ferrocenium–ferrocene. Potentials were determined in thf–0.2 mol dm^{-3} $[NBu_4][BF_4]$ at a vitreous carbon electrode, scan rate 100 mV s^{-1} at low temperature for the imides and at room temperature for the ylides. [b] Spectra in thf relative to $P(OMe)_3$. [c] Ylide complexes formed *in situ* by deprotonation of the parent imide. [d] Deprotonation of complex **9** or **10** gives the same ylide **11**.

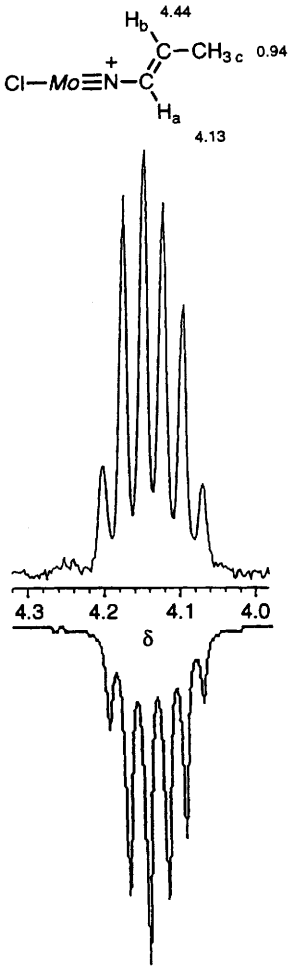

Fig. 3 Experimental NMR resonance of the vinylimide H_a proton of complex **10** centred at δ 4.13 and iterative simulation (below) of the peaks using a LAOCOON program.[7] Parameters: $^3J(H_aH_b)$ = 15.0, $^3J(H_bH_c)$ = 15.0, $^4J(H_aH_c)$ = 0.1 Hz; $^2J(H_cH_c)$ fixed at −12.0 Hz

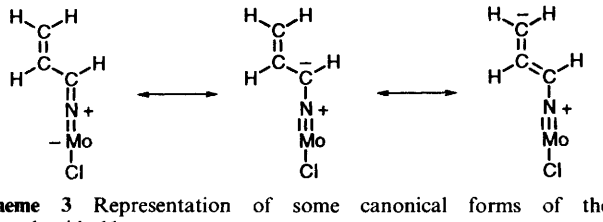

Scheme 3 Representation of some canonical forms of the alkenylamide **11**

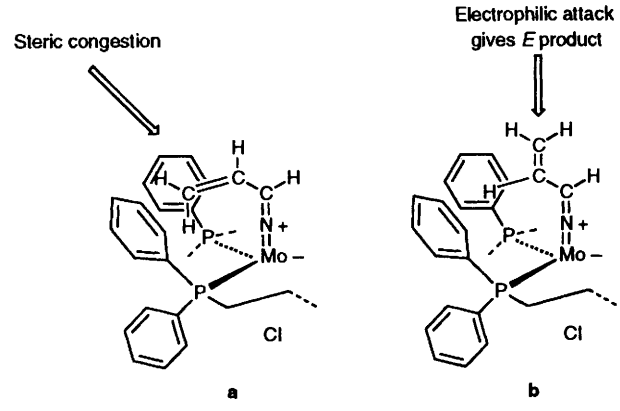

Scheme 4 Partial representation of conformers of complex **11** showing the unfavourable disposition of the CH_2 group (**a**) and the less-crowded configuration (**b**)

Formation of Cyanoformate Esters from trans-$[MoX(NCH_2CO_2R')(dppe)_2]^+$ (X = Cl *or* I, R' = Me *or* Et).—Mechanistic studies of the deprotonation of *trans*-$[MoCl(NCH_2CO_2Me)(dppe)_2]^+$ **1** showed that the electron-withdrawing ester group allowed the successive removal of *two* protons from the α-carbon by methoxide, thereby generating an anion possessing a co-ordinated cyanoformate ester group, Scheme 5.[5] Halide or nitrile ligands are known to be readily replaced by CO or N_2 at $\{Mo^0(dppe)_2\}$ centres.[10] This suggested that it might be possible to release cyanoformate esters and form stable molybdenum(0) complexes *via* substitution of the axial ligands in *trans*-$[MoX(NCCO_2R')(dppe)_2]^-$.

The complex *trans*-$[MoCl(NCCO_2Et)(dppe)_2]^-$ was generated in thf by treatment of **2** with an excess of $K[OBu^t]$ and the solution was stirred under an atmosphere of carbon monoxide for *ca.* 40 h. Work-up afforded $[Mo(CO)_2(dppe)_2]$ (*cis* and *trans* isomers) and the free ester $N{\equiv}C{-}CO_2Et$. The reaction of CO with the iodide *trans*-$[MoI(NCCO_2Et)(dppe)_2]^-$ gave the same products in somewhat better yield (*ca.* 80% yield of each). The corresponding reaction under molecular nitrogen gave *trans*-$[Mo(N_2)_2(dppe)_2]$ together with the free ester both in a yield of 60%. The isolated metal products were identified by infrared spectroscopy and cyclic voltammetry; $N{\equiv}C{-}CO_2Et$ was identified by infrared spectroscopy and HPLC. These results are summarised by Scheme 5 and details of the reactions are given in the Experimental section.

It seems likely that the cyanoformate ester and the molybdenum(0) products are formed by a sequence involving dissociative loss of the halide, binding of the π-acid ligand, dissociative loss of the cyanoformate ester and binding of the second π-acid ligand, as outlined in Scheme 5. Dissociative

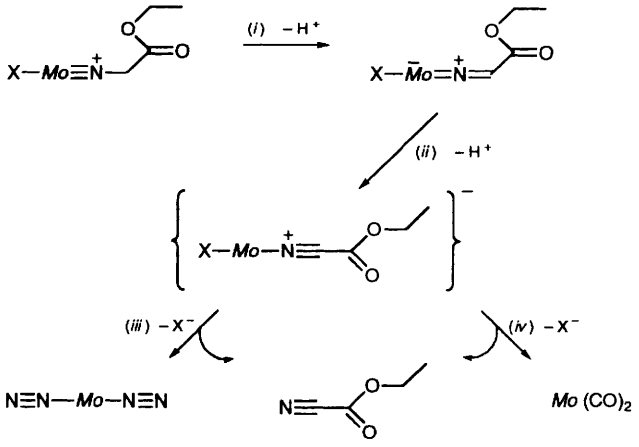

Scheme 5 Release of ethyl cyanoformate from an imide ester; *Mo* represents *trans*-{Mo(dppe)$_2$}. (*i*) NEt$_3$; (*ii*) $^-$OBu^t; (*iii*) N$_2$; (*iv*) CO

substitution reactions are well established at {Mo^0(dppe)$_2$} centres and halides tend to be more labile than nitrile ligands.[10] We have prepared *trans*-[Mo(N$_2$)(NCCO$_2$Et)(dppe)$_2$] and find that it reacts with dinitrogen at 1 atm (*ca.* 10^5 Pa) in thf to give *trans*-[Mo(N$_2$)$_2$(dppe)$_2$], as is consistent with this pathway.

Although [MoCl(NCCO$_2$Me)(dppe)$_2$]$^-$ protonates to regenerate the parent cation **1**, its reaction with MeI only gives the monomethylated product. Again, the steric demands of the dppe ligands must prevent formation of a tertiary α-carbon centre.

Formation of Glycine and DL-*Alanine Esters by Electroreductive Cleavage of* Mo–N *Bonds in trans*-[MoCl(NCHRCO$_2$Me)(dppe)$_2$]$^+$, (R = H *or* Me).—In earlier work it was shown that electrochemical reduction of the methylimide cation *trans*-[MoCl(NMe)(dppe)$_2$]$^+$ under dinitrogen in the presence of phenol gives methylamine and *trans*-[Mo(N$_2$)$_2$(dppe)$_2$] in an overall four-electron process.[11] We thought it should be possible to release glycine or DL-alanine methyl esters by an analogous reduction of *trans*-[MoCl(NCHRCO$_2$Me)(dppe)$_2$]$^+$.

Controlled-potential reductions of *trans*-[MoCl(NCH$_2$CO$_2$Me)(dppe)$_2$]$^+$ **1** were carried out at −2.3 V *versus* ferrocenium–ferrocene in thf–0.2 mol dm^{-3} [NBu$_4$][BF$_4$] at a mercury-pool cathode in the presence of phenol under molecular nitrogen. Coulometry showed that the electrode reaction consumed 1.3 F mol^{-1} of the starting material; cyclic voltammetry on the catholyte at the end of electrolysis revealed the formation of two metal products, *trans*-[Mo(N$_2$)$_2$(dppe)$_2$] and *trans*-[MoCl(NCHCO$_2$Me)(dppe)$_2$] **2** in yields of *ca.* 30 and *ca.* 60% respectively. Thin-layer chromatography and spectrophotometry confirmed the formation of the glycine ester in *ca.* 40% yield. The stoichiometry and charge consumption are broadly consistent with an overall reduction corresponding to that shown by Scheme 6 whereby the formation of **2** is explained by the sacrificial consumption of **1** as the proton source.

We sought to increase the yield of the amino acid ester by using a stronger acid than phenol, so as to circumvent the unproductive deprotonation step. Controlled-potential electrolysis of *trans*-[MoCl(NCHRCO$_2$Me)(dppe)$_2$]$^+$ in the presence of acetic acid led to the formation of glycine (R = H) or DL-alanine (R = Me) esters in yields of 70 and 80% respectively. The electrolysis involves a coupled dihydrogen evolution cycle which is catalysed by the metal product formed on release of the amino acid ester, Scheme 7.

Cyclic voltammetry of *trans*-[MoCl(NCHRCO$_2$Me)(dppe)$_2$]$^+$ in the presence of acetic acid shows the formation of the monohydride complex [MoH(η^2-O$_2$CMe)(dppe)$_2$] under dinitrogen or argon, Fig. 4. Under electrolysis conditions, monohydride formed at the electrode diffuses into the bulk solution where it is slowly protonated to give a dihydride cation

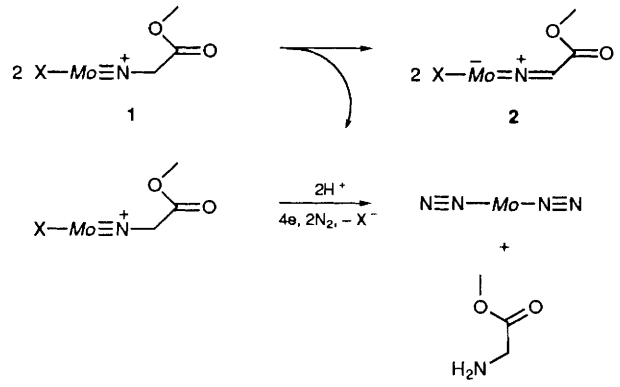

Scheme 6 Release of glycine methyl ester from complex **1** by electrolysis under dinitrogen; the sacrificial consumption of **1** provides the source of protons; *Mo* represents *trans*-{Mo(dppe)$_2$}

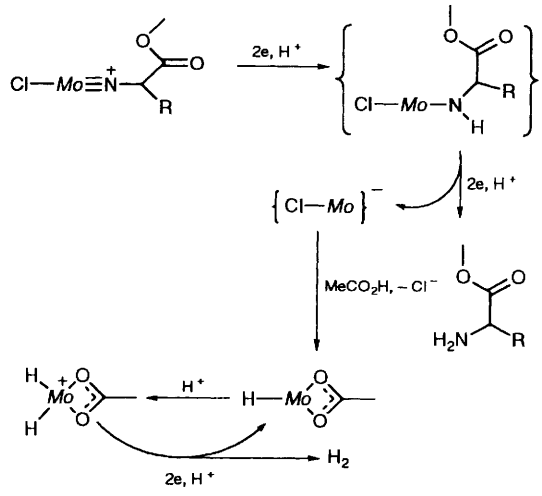

Scheme 7 Release of amino acid esters from imide esters by electrolysis in the presence of acetic acid. The species in brackets are postulated intermediates detected in related systems, see refs. 10 and 11. *Mo* represents *trans*-{Mo(dppe)$_2$}; R = Me or H

[MoH$_2$(η^2-O$_2$CMe)(dppe)$_2$]$^+$. The reduction of the dihydride occurs at a potential positive of that for the parent imide cation and an independent study has shown that this leads to the formation of a thermally unstable trihydride [MoH$_3$(η^1-O$_2$CMe)(dppe)$_2$].[12] Loss of H$_2$ from the trihydride regenerates [MoH(η^2-O$_2$CMe)(dppe)$_2$] which sustains the catalytic cycle.

Based upon this and earlier work[11] we suggest that the amino acid esters and metal products are formed by the pathway outlined in Scheme 7. Notably the monohydride is generated when either *trans*-[MoCl$_2$(dppe)$_2$], *trans*-[MoCl(NH)(dppe)$_2$]$^+$ or *trans*-[MoCl(O)(dppe)$_2$]$^+$ are reduced in the presence of acetic acid.

Cyclic voltammetry of the other organoimides reported herein shows that each undergoes reduction at a vitreous carbon electrode in thf–0.2 mol dm^{-3} [NBu$_4$][BF$_4$] and that their conjugate organoamides undergo facile oxidation, Table 5. The nature of the products formed by controlled-potential reduction or oxidation of these compounds is currently being investigated.

Conclusion

The reactions described herein begin to illustrate how a nucleophilic molybdenum nitride can be used to convert organic iodides into organonitrogen products. Changing the metal or the diphosphine coligands could extend the scope of such reactions. For example, increasing the nucleophilicity of

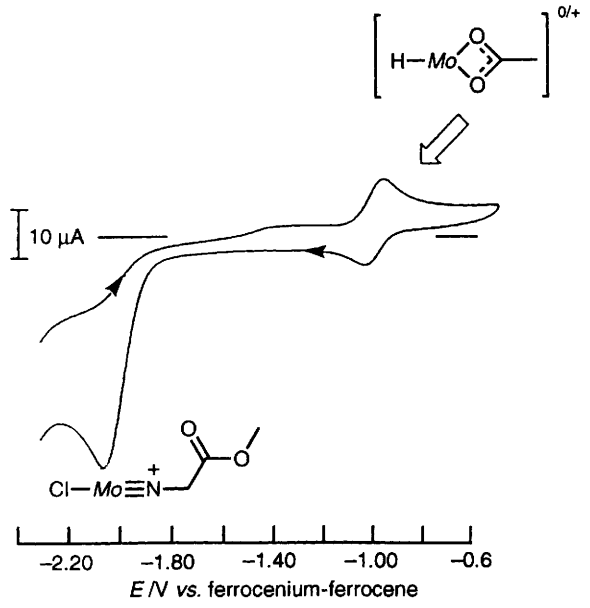

Fig. 4 Cyclic voltammogram of the imide complex **1** showing generation of the hydride upon holding the potential at −2.17 V for 20 s in the presence of acetic acid. Recorded in thf–0.2 mol dm^{-3} $[NBu_4][BF_4]$ at a vitreous carbon electrode, scan rate 100 m V s^{-1}

the ylide might allow carboxylation with CO_2; less sterically demanding diphosphine ligands might permit bulkier substituents to be introduced at the primary α-carbon and/or its conversion to a tertiary carbon centre.

Rather than behaving as merely 'spectator' ligands, it is becoming apparent that simple dppe coligands can exert stereochemical control over the reaction course of a group bound in an axial position: asymmetric diphosphine coligands might provide a route to chiral products and this is being investigated.

Experimental

All manipulations were carried under an inert atmosphere of dinitrogen or argon using Schlenk techniques. Solvents were freshly distilled from appropriate drying agents under dinitrogen. Alkyl iodides are best used freshly distilled under vacuum in the dark from K_2CO_3. The complexes *trans*-$[MoX(N)(dppe)_2]$ (X = Cl or Br) were prepared by the method of Chatt and Dilworth.[3]

The NMR measurements were made on a JEOL GSX MHz instrument, chemical shifts being given in ppm. Infrared spectra were recorded on a Bio-Rad 3240 FTS-7 FTIR spectrometer. Spectrophotometric measurements were performed on a Perkin-Elmer Lamda 5 spectrophotometer. The HPLC analyses were made using a JASCO 880-PU pump and a Shimadzu SPD-SA UV detector. Mass spectra (FAB and electron impact, EI) were obtained using an Analytical Fison Instruments Auto Spec VG spectrometer; FAB spectra were generated using 3-nitrobenzyl alcohol as the matrix.

Cyclic voltammetric and controlled-potential electrolysis experiments were carried out using a Hi-Tek DT 2101 potentiostat interfaced with a Hi-Tek PPR1 waveform generator and data were recorded on a Philips PM 8041 X-Y recorder. Coulometric measurements were made using an electronic integrator supplied by Southampton University. Three electrode–two compartment cells equipped with vitreous carbon-disc or platinum-wire working electrodes, a tungsten-wire secondary electrode and a silver-wire pseudo-reference electrode or a calomel reference electrode were employed for cyclic voltammetric measurements. The concentrations of the complexes were typically 1–2 mmol dm^{-3} and 0.2 mol dm^{-3} $[NBu_4][BF_4]$ was used as the supporting electrolyte in thf or other solvents. Controlled-potential electrolyses were made in an H-type cell with a three-electrode–three compartment configuration as detailed below.

Microanalyses (C, H, N) were made in house or by the Department of Chemistry, University of Surrey.

trans-$[MoCl(NEt)(dppe)_2][BPh_4]$ **6**.—The complex *trans*-$[MoCl(N)(dppe)_2]$ (1.1 g, 1.2 mmol) was dissolved in thf (70 cm^3) at room temperature. An excess of EtI (1 cm^3) was added and the reaction mixture stirred overnight. During this time the solution changed from yellow to reddish pink and some pink solid precipitated. The solution was reduced in volume to *ca.* 5 cm^3 and the pink solid filtered off. The solid was extracted twice with CH_2Cl_2. The combined extract was evaporated to dryness and the solid washed with cold thf (3 × 5 cm^3) then Et_2O (2 × 5 cm^3) and dried *in vacuo* giving *trans*-$[MoCl(NEt)(dppe)_2]I$ (0.91 g, 70% yield). The product was dissolved in MeOH (30 cm^3) and an excess of $NaBPh_4$ was added to the stirred solution. Bright pink *trans*-$[MoCl(NEt)(dppe)_2][BPh_4]$ precipitated. This was filtered off, washed with MeOH (3 × *ca.* 3 cm^3), Et_2O (3 × *ca.* 3 cm^3) and dried *in vacuo*. FAB mass spectrum *m/z* 972 (M^+) [Found (Calc. for $C_{78}H_{73}BClMoNP_4$): C, 71.8 (72.6); H, 5.70 (5.70); N, 1.2 (1.1)%]. NMR (CD_2Cl_2): ^1H (relative to $SiMe_4$, 270.16 MHz), δ −2.04 (t, 3 H, CH_3), 1.855 (m, 2 H, NCH_2), 2.6–2.9 (two br m, 8 H, PCH_2CH_2P) and 6.8–7.5 (m, 60 H, PPh and BPh); ^{31}P-$\{^1H\}$ (relative to trimethyl phosphite, 109.25 MHz), δ −97.0.

trans-$[MoCl(NCH_2CH{=}CH_2)(dppe)_2][PF_6]$ **9**.—Pink *trans*-$[MoCl(NCH_2CH{=}CH_2)(dppe)_2]I$ was synthesised in 80% yield from the nitride and allyl iodide by the procedure described above. It was converted into the $[PF_6]^-$ salt with $Tl[PF_6]$ (**CAUTION**: poison) or to the $[BPh_4]^-$ salt as before. FAB mass spectrum: *m/z* 984 (M^+) [Found (Calc. for $C_{55}H_{53}ClF_6MoNP_5$): C, 58.1 (58.6); H 4.9 (4.7); N 1.3 (1.2)%]. NMR (CD_2Cl_2) for $[BPh_4]^-$ salt: ^1H (270.16 MHz), δ 2.35 (d, 2 H, NCH_2), 2.6–2.9 (two br m, 8 H, PCH_2CH_2P), 4.24 (m, 2 H, $CH_2{=}CH$), 4.62 (m, 1 H, $CH_2{=}CHCH_2$) and 6.8–7.5 (m, 60 H, PPh and BPh); ^{31}P-$\{^1H\}$ (109.25 MHz), δ −96.8 (s).

trans-$[MoCl(NCH_2CO_2Me)(dppe)_2]I$ **1**.—The complex *trans*-$[MoCl(N)(dppe)_2]$ (0.45 g, 0.48 mmol) was dissolved in thf (30 cm^3) at room temperature, ICH_2CO_2Me (0.27 cm^3, 0.75 mmol) was added and the reaction mixture stirred overnight. A violet solid precipitated which was filtered off, washed with thf (2 × 5 cm^3) then Et_2O (2 × 5 cm^3) and dried *in vacuo*. Yield 0.36 g, 65%. Recrystallisation from CH_2Cl_2–Et_2O afforded violet needles [Found (Calc. for $C_{55}H_{53}ClIMoNO_2P_4$): C, 56.5 (56.2); H, 4.6 (4.6); N, 1.3 (1.2)%]. NMR (CD_2Cl_2): ^1H (270.16 MHz) δ 2.65 (2 H, NCH_2) 2.8–3.1 (br m, 8 H, PCH_2CH_2P) superimposed with 3.08 (3 H, s, OCH_3) and 6.5–7.5 (m, 40 H, PPh); ^{31}P-$\{^1H\}$ (109.25 MHz), δ −98.0 (s); ^{13}C-$\{^1H\}$ ($SiMe_4$), δ 27.3 (q, PCH_2), 52.5 (s, OCH_3), 63.3 (s, NCH_2), 128–135 (m, PPh) and 164.4 (s, CO). FTIR (Nujol mull, $\tilde{\nu}/cm^{-1}$): 1753s [ν(CO)].

trans-$[MoCl(NCH_2CO_2Et)(dppe)_2]I$.—The complex was prepared as a violet solid in 71% yield using ICH_2CO_2Et by the procedure described above and was converted into the $[PF_6]^-$ salt by cation exchange with $[NH_4][PF_6]$ in thf and recrystallised from CH_2Cl_2–Et_2O as violet needles [Found (Calc. for $C_{55}H_{55}ClF_6MoNO_2P_5{\cdot}0.5CH_2Cl_2$): C, 55.3 (55.8); H, 4.4 (4.6); N, 1.4 (1.1)%]. NMR: ^1H ($CDCl_3$, 270.16 MHz), δ 0.9 (t, OCH_2CH_3), 2.7 (m, 2 H, NCH_2), 3.4 (q, 2 H, OCH_2); 2.9–3.2 (br m, 8 H, PCH_2CH_2P) and 7.1–7.6 (m, 40 H, PPh); ^{31}P-$\{^1H\}$ (CD_2Cl_2, 109.25 MHz), δ −98.7 (s, MoP) and −285 (qnt, PF_6) FTIR (Nujol mull, $\tilde{\nu}/cm^{-1}$): 1756s [ν(CO)], 840 and 560s [ν(PF)].

trans-$[MoI(NCH_2CO_2Et)(dppe)_2]I$.—This complex was prepared in 62% yield from *trans*-$[MoI(N)(dppe)_2]$ as

described above and converted into the $[PF_6]^-$ salt [Found (Calc. for $C_{56}H_{55}F_6IMoNO_2P_5 \cdot 0.5CH_2Cl_2$): C, 53.6 (53.1); H, 4.8 (4.4); N, 1.5 (1.1)%]. ^1H NMR ($CDCl_3$, 270.16 MHz): δ 0.9 (t, 3 H, OCH_2CH_3), 2.7 (m, 2 H, NCH_2), 3.4 (q, 2 H, OCH_2), 2.9–3.2 (br m, 8 H, PCH_2CH_2P) and 7.1–7.6 (m, 40 H, PPh). FTIR (Nujol mull, $\tilde{\nu}/cm^{-1}$): 1745s [ν(CO)], 840 and 560s [ν(PF)].

trans-[MoCl(NCHCO$_2$Me)(dppe)$_2$] **2**.—The complex *trans*-[MoCl(NCH$_2$CO$_2$Me)(dppe)$_2$]I (0.2 g, 0.175 mmol) was dissolved in CH_2Cl_2 (20 cm^3) and NEt_3 (0.5 cm^3) added to the violet solution. The colour changed immediately to greenish yellow. The volume was reduced to about 5 cm^3, an equal volume of MeOH was added and the solution was left to stand overnight. Well formed dark green crystals deposited which were filtered off, copiously washed with methanol and dried *in vacuo*. Yield (0.16 g, 90%) [Found (Calc. for $C_{55}H_{52}ClMoNO_2P_4 \cdot 0.5CH_2Cl_2$): C, 63.1 (63.1); H, 5.2 (5.1); N, 1.3 (1.5)%]. NMR (CD_2Cl_2): ^1H (270.16 MHz); δ 3.28 (qnt, 1 H, NCH), 2.65–2.8 (2 × br m, 8 H, PCH_2CH_2P), 3.00 (3 H, s, OCH_3) and 6.5–7.5 (m, 40 H, PPh); ^{31}P-{^1H} (109.25 MHz), δ −86.7 (s). FTIR (Nujol mull, $\tilde{\nu}/cm^{-1}$): 1607, 1622 and 1637s [ν(CO), ν(C=N)].

trans-[MoCl{NCH(Me)CO$_2$Me}(dppe)$_2$]I **3**.—The complex *trans*-[MoCl(NCHCO$_2$Me)(dppe)$_2$] (0.165 g, 0.16 mmol) was dissolved in thf (25 cm^3) and MeI (0.5 cm^3) added. The solution was stirred for 48 h and a pale violet solid precipitated. The solid was filtered off, washed with thf, dried *in vacuo* and recrystallised from warm MeCN as violet needles. Yield 0.14 g, 74% [Found (Calc. for $C_{56}H_{55}ClIMoNO_2P_4$): C, 57.9 (58.2); H, 4.9 (4.8); N, 1.2 (1.2)%]. NMR (CD_2Cl_2): ^1H (270.16 MHz), δ 0.27 (d, 3 H, NCH*Me*), 2.87 (3 H, s, OCH_3), 2.9–3.1 [2 × br m, 9 H, PCH_2CH_2P superimposed with NC*H*Me (irradiation at δ 3.0 causes collapse of doublet at δ 0.27 to a singlet)] and 6.5–7.5 (m, 40 H, PPh); ^{31}P-{^1H} (109.25 MHz), δ −99.4 (s); ^{13}C-{^1H}, δ 18.2 (s, NCH*Me*), 26.8 and 27.5 (m, PCH_2), 52.8 (s, OCH_3), 70.9 (s, NCH), 128–135 (m, PPh) and 167.5 (s, CO). FTIR (Nujol mull, $\tilde{\nu}/cm^{-1}$): 1748s [ν(CO)].

trans-[MoCl(NCHMe$_2$)(dppe)$_2$][BPh$_4$] **8**.—The complex *trans*-[MoCl(NEt)(dppe)$_2$][BPh$_4$] (0.1 g, 0.08 mmol) was partially dissolved in thf (30 cm^3) and solid K[OBu^t] (0.026 g, 0.23 mmol) was added to the stirred suspension. A clear orange solution of *trans*-[MoCl(NCHMe)(dppe)$_2$] rapidly formed to which MeI (0.3 cm^3) was then added and the solution stirred overnight at room temperature. The volume of the solution was reduced to 5 cm^3 and cooled in ice. The pink solid was filtered off and extracted with the minimum volume of CH_2Cl_2. The filtered extract was taken to dryness and washed with cold thf (3 × 5 cm^3), MeOH (3 × 5 cm^3), Et_2O (3 × 5 cm^3) and dried *in vacuo*. Yield of pink *trans*-[MoCl(NCHMe$_2$)(dppe)$_2$][BPh$_4$] 50%. FAB mass spectrum: *m*/*z* 986 (M^+) [Found (Calc. for $C_{79}H_{75}BClMoNP_4$): C, 72.9 (72.7); H, 6.5 (5.8); N, 1.1 (1.1)%]. NMR (CD_2Cl_2): ^1H (270.16 MHz); δ −0.12 (d, 6 H, CH_3, J = 6.7), 2.48 [m, 1 H, NC*H*Me$_2$, J = 6.7 Hz], 2.6–2.9 (two br m, 8 H, PCH_2CH_2P) and 6.8–7.5 (m, 60 H, PPh and BPh); ^{31}P-{^1H} (109.25 MHz), δ −98.1 (s).

trans-[MoCl(NBu)(dppe)$_2$][BPh$_4$] **7**.—This compound was prepared in 70% yield by the reaction of deprotonated *trans*-[MoCl(NMe)(dppe)$_2$][BPh$_4$] with *n*-propyl iodide following an analogous procedure to that described above. The pink product was recrystallised from CH_2Cl_2–Et_2O. FAB mass spectrum: *m*/*z* 1000 (M^+) [Found (Calc. for $C_{80}H_{77}BClMoNP_4 \cdot 0.5CH_2Cl_2$): C, 70.6 (71.0); H, 6.3 (5.8); N, 1.1 (1.0)%].

Complex **6** was made in *ca.* 70% yield from *trans*-[MoCl(NMe)(dppe)$_2$][BPh$_4$] and MeI following the same procedure; spectroscopic data identical to the sample prepared by ethylation of the nitride as described above.

trans-[MoCl(NCH=CHMe)(dppe)$_2$][BPh$_4$] **10**.—Solid K[OBu^t] (0.04 g, 0.34 mmol) was added to a stirred suspension of *trans*-[MoCl(NCH$_2$CH=CH$_2$)(dppe)$_2$]I (0.12 g, 0.11 mmol) in thf (30 cm^3) and a deep orange solution of the intermediate *trans*-[MoCl(N=CHCH=CH$_2$)(dppe)$_2$] was rapidly formed. At room temperature, $HBF_4 \cdot OEt_2$ (*ca.* 50% in Et_2O, 0.1 cm^3) was added to the stirred solution, which changed from orange to pale red. The reaction mixture was stirred for 1 h and the solution filtered through Celite to remove KI. The filtrate was evaporated to dryness and extracted with the minimum volume of CH_2Cl_2, filtered, evaporated to dryness and taken up in the minimum volume of methanol. Addition of $NaBPh_4$ (*ca.* 0.2 g) to the methanolic solution precipitated the product as the $[BPh_4]^-$ salt which was filtered off and recrystallised from CH_2Cl_2–Et_2O as a metallic silver-rose microcrystalline solid in 55% yield. FAB Mass spectrum. *m*/*z* 984 (M^+) [Found (Calc. for $C_{79}H_{73}BClMoNP_4 \cdot 0.25CH_2Cl_2$): C, 71.8 (71.9); H, 5.8 (5.6); N, 1.1 (1.1%)]. NMR (CD_2Cl_2): ^1H (270.16 MHz) δ 0.94 [d, 3 H, $CHCH_3$, J_{H-Me} = 7], 2.6–2.9 (2 × m, 8 H, PCH_2CH_2P) 4.13 [sxt, 1 H, NCH=C*H*Me, J_{trans} = 15, J_{H-Me} = 7] 4.44 [dm, 1 H, NC*H*=CHMe, J_{trans} = 15 Hz] and 6.8–7.5 (m, 60 H, PPh and BPh); ^{31}P-{^1H} (109.25 MHz), δ −97.2 (s).

trans-[MoCl(NCH=CHEt)(dppe)$_2$][BPh$_4$] **12**.—This complex was prepared in an analogous fashion to the methyvinylimide by addition of MeI (*ca.* 0.3 cm^3) to the deprotonated allylimide and stirring the reaction mixture overnight. Work-up as before and recrystallisation from thf–Et_2O gave the silver-rose microcrystalline product in 50% yield. FAB mass spectrum: *m*/*z* 998 (M^+) [Found (Calc. for $C_{80}H_{75}BClMoNP_4$): C, 73.9 (73.0); H, 6.0 (5.8); N, 1.2 (1.1%)]. ^1H NMR (CD_2Cl_2): ^1H (270.16 MHz), δ 0.53 (t, 3 H, CH_2CH_3, J = 7.4), 1.32 (qnt, 2 H, CH_2CH_3, J = 6.5 and 7.4 Hz) 2.6–2.9 (2 × br m, 8 H, PCH_2CH_2P), 4.26 (qnt, 1 H, CH=C*H*CH$_2$), 4.40 (dm, 1 H, NC*H*=CH), and 6.8–7.5 (m, 60 H, PPh and BPh); ^{31}P-{^1H} (109.25 MHz), δ −97.7 (s).

Formation of Cyanoformic acid Ethyl Ester, NCCO$_2$Et.—The complex *trans*-[MoI(NCH$_2$CO$_2$Et)(dppe)$_2$]I (0.17 g, 0.14 mmol) was suspended in thf (40 cm^3) and solid K[OBu^t] (0.07 g, 0.57 mmol) was added to the stirred solution which rapidly changed from pale violet to green. Dinitrogen was passed through the stirred solution for 44 h during which time it changed to orange-red. Concentration of the solution to a small volume gave orange microcrystalline *trans*-[Mo(N$_2$)$_2$(dppe)$_2$] which was filtered off, washed with MeOH and dried *in vacuo*. Yield = 0.076 g, 0.08 mmol (57%); ν(N$_2$) 1980 cm^{-1} (Nujol mull); $E_{\frac{1}{2}}^{ox}$ = 0.70 V *versus* ferrocenium–ferrocene. Addition of Et_2O to the filtrate precipitated a small amount of unidentified green material which was filtered off. The filtrate was transferred to a volumetric flask, diluted to volume with thf and analysed by HPLC using a Merck–LIChroCart 250-4 RP 18, 5 μm column. The sole organic product was identified as NCCO$_2$Et formed in 55% yield. Its identity was confirmed by evaporation of the filtrate and liquid-film IR spectroscopy. Strong bands observed at ν(CN) 2250 cm^{-1} and ν(CO) 1743 cm^{-1} are identical to those of an authentic sample.

The procedure was repeated except that carbon monoxide rather than dinitrogen was passed through the solution. The complex [Mo(CO)$_2$(dppe)$_2$] (*cis* and *trans* isomers) was formed and isolated as a yellow solid in 80% yield. Also HPLC showed that NCCO$_2$Et was formed in 80% yield; the green by-product was not obtained under these conditions. Repeating the same experiment under CO but employing *trans*-[MoCl(NCH$_2$CO$_2$Et)(dppe)$_2$]I rather than the iodo-complex, gave the same products but in somewhat lower yields (70% complex, 70% ester).

trans-[Mo(N$_2$)(NCCO$_2$Et)(dppe)$_2$].—This complex was prepared by modifying the general method of Hidai and co-workers[10] for related nitrile complexes. The complex *trans*-

Table 6 Crystal data and results of structure analyses

	2	**3a**	**3b**
Elemental formula	$C_{55}H_{52}ClMoNO_2P_4{\cdot}CH_2Cl_2$	$C_{56}H_{55}ClIMoNO_2P_4{\cdot}2C_2H_3N{\cdot}C_4H_8O$	$C_{56}H_{55}ClIMoNO_2P_4{\cdot}C_2H_3N$
M	1099.2	1310.5	1197.3
Crystal system	Monoclinic	Triclinic	Monoclinic
Space group (no.)	$C2$ (no. 5)	$P\bar{1}$ (no.2)	$P2_1/n$ (equiv. to no. 14)
a/Å	21.851(3)	12.610(1)	19.378(2)
b/Å	14.054(2)	13.207(1)	17.408(2)
c/Å	17.152(1)	19.774(2)	17.063(2)
α/°		109.036(7)	
β/°	101.259(9)	100.833(7)	106.756(7)
γ/°		99.916(8)	
U/Å^3	5165.9(10)	2959.3(5)	5511.2(9)
Z	4	2	4
D_c/g cm^{-3}	1.413	1.471	1.443
$F(000)$	2264	1340	2432
μ(Mo-Kα) cm^{-1}	5.7	9.3	9.9
Crystal colour, shape	Deep red diamond prisms	Small red plates	Large red rectangular prisms
Crystal size/mm	0.12 × 0.21 × 0.26	0.14 × 0.21 × 0.33	0.29 × 0.36 × 0.50
Crystal mounting	On glass fibre	Coated in epoxy resin	On glass fibre
θ_{max} for intensities/°	23	22	25
Crystal degradation (%)	0	5.3	3.0
Total no. of unique reflections	3767	7236	9661
No. of observed reflections $I > 2\sigma_I$	3105	5065	6121
Final R, R_g[13]	0.060, 0.062	0.072, 0.089	0.089, 0.088
No. of reflections used	3411 ($I < 1.5\sigma_I$)	6306 ($I < \sigma_I$)	9569 (all but 2)
g In weighting scheme	0.000 47	0.002 72	0.0015
Final difference map higest peaks/e Å^{-3}	0.45, near major solvent molecule	0.97, close to iodide	1.7, close to Mo

* $w = (\delta_F{}^2 + gF^2)^{-1}$.

$[Mo(N_2)_2(dppe)_2]$ (0.23 g, 0.24 mmol) was dissolved in thf (40 cm^3) and ethyl cyanoformate (0.1 cm^3, 1.0 mmol) added to the stirred solution. The reaction mixture was irradiated for 4.5 h with a tungsten-filament lamp (300 W) during which time it changed from orange to red. Concentration of the solution under vacuum afforded a red precipitate which was filtered off, washed with Et_2O and dried *in vacuo*. Recrystallisation from thf–Et_2O gave the product as a red microcrystalline solid (0.13 g, 0.13 mmol) in 53% yield [Found (Calc. for $C_{52}H_{45}MoN_3P_4$): C, 65.8 (65.8); H, 5.5 (5.2); N, 4.1 (4.1)%]. ^{1}H NMR (CD_2Cl_2, 270.16 MHz): δ 1.05 (t, 3 H, CH_2CH_3) 3.30 (q, 2 H, OCH_2CH_3) 2.7–3.1 (2 × br m, 8 H, PCH_2CH_2P) and 6.8–7.5 (m, 40 H, PPh). FTIR (Nujol mull, $\tilde{\nu}$/cm^{-1}): 1710s [ν(CO)]; 2094s [$\nu(N_2)$] and 2170w [ν(CN)].

trans-$[Mo(N_2)(NCCO_2Et)(dppe)_2]$ (0.09 g, 0.08 mmol) was stirred under dinitrogen in thf for 15 h. Removal of the solvent under vacuum and examination of the residue by FTIR spectroscopy (Nujol mull, $\tilde{\nu}$/cm^{-1}) showed the formation of the free ester, 1744s, [ν(CO)] and 2247w [ν(CN)], *trans*-$[Mo(N_2)_2(dppe)_2]$ (1997) together with the unreacted starting material. The formation of *trans*-$[Mo(N_2)_2(dppe)_2]$ was also confirmed by cyclic voltammetric experiments in thf–0.2 mol dm^{-3} $[NBu_4][BF_4]$ at Pt: the reversible oxidation process for *trans*-$[Mo(N_2)(NCCO_2Et)(dppe)_2]$ at $E_{\frac{1}{2}} = -0.44$ V *versus* ferrocenium–ferrocene was gradually replaced by that for *trans*-$[Mo(N_2)_2(dppe)_2]$ ($E_{\frac{1}{2}} = -0.70$ V) on purging the solution with dinitrogen.

Formation of Glycine and DL-*Alanine Methyl Esters*.—The complex *trans*-$[MoCl(NCH_2CO_2Me)(dppe)_2]I$ (0.08 g, 0.07 mmol) was dissolved in thf–0.2 mol dm^{-3} $[NBu_4][BF_4]$ (*ca.* 15 cm^3) which was contained in the working-electrode compartment of the H-type electrochemical cell. Glacial acetic acid (1.5 cm^3) was added to the solution of the complex. Electrolysis was carried out under argon at a vitreous carbon cathode of nominal area 2 cm^2 at an applied potential of −2.3 V *versus* ferrocenium–ferrocene. The catholyte was stirred at an even rate during electrolysis using a magnetic follower and the current was monitored continuously as a function of the charge passed. The solution changed during electrolysis from pink through red to a deep orange and the current decayed to a steady-state value. The electrolysis was terminated after the passage of 5F mol^{-1} of charge and the orange solution removed from the cell by a gas-tight syringe. On standing for *ca.* 0.5 h the solution changed to bright magenta as $[MoH(\eta^2\text{-}O_2CMe)(dppe)_2]$ was slowly converted into $[MoH_2(\eta^2\text{-}O_2CMe)(dppe)_2]^+$. The formation of the glycine ester was confirmed by TLC and quantified colorimetrically with ninhydrin,[13] yield based on complex = 70%, current yield = 56%. Alanine methyl ester was electrosynthesised by the same procedure, yield based on complex = 80%, current yield = 64%.

Crystal Structure Analyses.—The analyses of three crystals are reported, of compound **2** and of two forms of compound **3** (**a** and **b**). The procedures followed for **2** are described; those for **3** were very similar. Crystal data and details of the analyses are in Table 6.

Crystals of complex **2** range from red to very dark red; some were dichroic red-green. One was mounted on a glass fibre and, after photographic examination, transferred to an Enraf-Nonius CAD4 diffractometer [with monochromated radiation, λ(Mo-Kα) = 0.710 69 Å] for determination of accurate cell dimensions (from the settings of 25 reflections, θ *ca.* 10.5°, each reflection centred in four orientations) and for measurement of diffraction intensities. During processing, the intensities were corrected for Lorentz-polarisation effects and adjusted by Bayesian statistical methods to ensure no negative net values. No corrections for crystal deterioration or absorption were applied [N.B. crystals **3a** and **3b** both showed slight deterioration; corrections for absorption (by semiempirical ψ-scan methods) were applied to **3b**].

The structure of complex **2** was determined by the heavy-atom method in the SHELX system;[14] **3b** was solved similarly,

but **3a** required use of the automated Patterson routines in SHELXS.[15] Refinement was by large-block-matrix least-squares methods with all principal atoms allowed anisotropic thermal parameters. Hydrogen atoms in the diphosphine ligands were included in idealised positions. Refinement of the inverted structure showed no significant differences. There is disorder of the ClMo(amide) group and of the CH_2Cl_2 solvent molecule which lies close to the chloride ligand; this grouping lies in opposing directions, in the ratio of *ca.* 4:1, in the major and minor components in the crystal. The atoms in the minor component [except for Mo′ and Cl(5′)] were refined isotropically. In the final difference map there was a peak where we would have expected to find H(61), in the plane of the amide ligand; the atom was not included in the structure-factor calculation but is shown in Fig. 1(*a*).

There is disorder also in the crystals of both **3a** and **3b**. In **3a** one of the two acetonitrile molecules is disordered over several orientations and the 'solvent' molecule (believed to be thf) is poorly resolved; the cation appears well resolved and it is this structure that has been described elsewhere. The hydrogen atoms in the imide ligand were included in calculated positions; those of the methyl groups were allowed to refine with geometrical constraints. Crystal **3b** shows disorder in the acetonitrile molecule and in the imide ligand; either enantiomer can be accommodated equally, such that the N(6), C(62), O(63) and C(64) atom sites are common (or very nearly so) to both enantiomers, with the other atoms either side of a pseudo-mirror plane.

Scattering factor curves for neutral atoms were taken from ref. 16. Computer programs used in the analyses have been noted above and in Table 4 of ref. 17, and were run on a DEC MicroVAX 3600 machine in the Nitrogen Fixation Laboratory.

Additional material available from the Cambridge Crystallographic Data Centre comprises H-atom coordinates, thermal parameters and remaining bond lengths and angles.

Acknowledgements

We gratefully thank Dr. Ali Abdulsadda of the School of Chemistry and Molecular Science, University of Sussex, for FAB mass spectral measurements. The Calouste Gulbenkian Foundation and the Universidade do Minho are thanked for providing travel funds for A. F.

References

1 D. L. Hughes, S. K. Ibrahim, C. J. Macdonald, H. Moh'd Ali and C. J. Pickett, *J. Chem. Soc., Chem. Commun.*, 1992, 1762.
2 W. Hussain, G. J. Leigh and C. J. Pickett, *J. Chem. Soc., Chem. Commun.*, 1982, 747; R. A. Henderson, G. J. Leigh and C. J. Pickett, *J. Chem. Soc., Dalton Trans.*, 1989, 425.
3 J. Chatt and J. R. Dilworth, *J. Chem. Soc., Chem. Commun.*, 1975, 983; *J. Indian Chem. Soc.*, 1977, **54**, 13; R. A. Henderson, G. Davies, J. R. Dilworth and R. N. F. Thorneley, *J. Chem. Soc., Dalton Trans.*, 1981, 40; P. C. Bevan, J. Chatt, J. R. Dilworth and G. J. Leigh, *J. Chem. Soc., Dalton Trans.*, 1982, 821; D. L. Hughes, M. Y. Mohammed and C. J. Pickett, *J. Chem. Soc., Dalton Trans.*, 1990, 2013.
4 D. L. Hughes, M. Y. Mohammed and C. J. Pickett, *J. Chem. Soc., Chem. Commun.*, 1989, 1399; A. Hills, D. L. Hughes, C. J. Macdonald, M. Y. Mohammed and C. J. Pickett, *J. Chem. Soc., Dalton Trans.*, 1991, 121; C. J. Pickett, *NATO ASI Ser. C*, 1993, **385**, 357; D. L. Hughes, S. K. Ibrahim, C. J. Macdonald, H. Moh'd Ali and C. J. Pickett, *J. Chem. Soc., Chem. Commun.*, 1994, 425.
5 R. A. Henderson, S. K. Ibrahim and C. J. Pickett, *J. Chem. Soc., Chem. Commun.*, 1993, 392.
6 D. L. Hughes, D. J. Lowe, M. Y. Mohammed, C. J. Pickett and N. M. Pinhal, *J. Chem. Soc., Dalton Trans.*, 1990, 2021; M. T. Duarte, J. J. R. Frausta da Silva, A. M. Galvao, M. C. Guedes da Silva, P. B. Hitchcock, D. L. Hughes, C. J. Pickett, A. J. L. Pombeiro, R. L. Richards and T. I. Al-Salih, *J. Chem. Soc., Dalton Trans.*, 1993, 3015.
7 LAOCOON, based on original LAOCN3 program, A. Bothner-By and S. M. Castallans, Computer Programs for Chemistry, ed. D. F. Tar, Benjamin Inc., New York, 1968.
8 Y. Ishi, H. Miyagi and M. Hidai, *J. Chem. Soc., Chem. Commun.*, 1990, 1569; Y. Ishi, H. Miyagi, S. Jitsukuni, H. Seino, B. S. Harkness and M. Hidai, *J. Am. Chem. Soc.*, 1992, **114**, 9890.
9 W. Hussain, G. J. Leigh, H. Moh'd. Ali and C. J. Pickett, *J. Chem. Soc., Dalton Trans.*, 1986, 1473.
10 T. Tatsumi, M. Hidai and Y. Uchida, *Inorg. Chem.*, 1975, **14**, 2530; T. I. Al-Salih and C. J. Pickett, *J. Chem. Soc., Dalton Trans.*, 1985, 1255; J. Chatt, R. A. Head, G. J. Leigh and C. J. Pickett, *J. Chem. Soc., Dalton Trans.*, 1977, 1638.
11 M. Y. Mohammed and C. J. Pickett, *J. Chem. Soc., Chem. Commun.*, 1988, 1119.
12 D. L. Hughes, S. K. Ibrahim, G. Querne, A. Laouenan, J. Talarmin, M. A. Queiros, A. Fonseca and C. J. Pickett, *Polyhedron*, 1994, **13**, 3341.
13 J. R. Spies, *Methods Enzymol.*, 1957, **3**, 468.
14 G. M. Sheldrick, SHELX, Program for crystal structure determination, University of Cambridge, 1976.
15 G. M. Sheldrick, *Acta Crystallogr., Sect. A*, 1990, **46**, 467.
16 *International Tables for X-Ray Crystallography*, Kynoch Press, Birmingham, 1974, vol. 4, pp. 99 and 149.
17 S. N. Anderson, R. L. Richards and D. L. Hughes, *J. Chem. Soc., Dalton Trans.*, 1986, 245.

Received 21*st December* 1994; *Paper* 4/07766K